

Analysis of $B \rightarrow a_1(1260)(b_1(1235))K^*$ decays in the perturbative QCD approach

Zhi-Qing Zhang

*Department of Physics, Henan University of Technology,
Zhengzhou, Henan 450052, P.R.China*

(Dated: June 24, 2018)

Abstract

Within the framework of perturbative QCD approach, we study the charmless two-body decays $B \rightarrow a_1(1260)K^*, b_1(1235)K^*$. Using the decays constants and the light-cone distribution amplitudes for these mesons derived from the QCD sum rule method, we find the following results: (a) Our predictions for the branching ratios are consistent well with the QCDF results within errors, but much larger than the naive factorization approach calculation values. (b) We predict that the anomalous polarizations occurring in the decays $B \rightarrow \phi K^*, \rho K^*$ also happen in the decays $B \rightarrow a_1 K^*$, while do not happen in the decays $B \rightarrow b_1 K^*$. Here the contributions from the annihilation diagrams play an important role to explain the larger transverse polarizations in the decays $B \rightarrow a_1 K^*$, while they are not sensitive to the polarizations in decays $B \rightarrow b_1 K^*$. (c) Our predictions for the direct CP-asymmetries agree well with the QCDF results within errors. The decays $\bar{B}^0 \rightarrow b_1^+ K^{*-}, B^- \rightarrow b_1^0 K^{*-}$ have larger direct CP-asymmetries, which could be measured by the present LHCb experiments.

PACS numbers: 13.25.Hw, 12.38.Bx, 14.40.Nd

I. INTRODUCTION

In general, the mesons are classified in J^{PC} multiplets. There are two types of orbitally excited axial-vector mesons, namely, 1^{++} and 1^{+-} . The former includes $a_1(1260)$, $f_1(1285)$, $f_1(1420)$, and K_{1A} , which compose the 3P_1 nonet, and the latter includes $b_1(1235)$, $h_1(1170)$, $h_1(1380)$, and K_{1B} , which compose the 1P_1 nonet. There is an important characteristic of these axial-vector mesons, with the exception of $a_1(1260)$ and $b_1(1235)$, that is, each different flavor state can mix with another one, which comes from the other nonet meson or the same nonet. There is not a mix between $a_1(1260)$ and $b_1(1235)$ because of the opposite C parities. They do not also mix with others. So compared with other axial-vector mesons, these two mesons should have less uncertainties regarding their inner structures.

Like the decay modes $B \rightarrow VV$, the charmless decays $B \rightarrow a_1(1260)K^*$, $b_1(1235)K^*$ also have three polarization states and so are expected to have rich physics. In many $B \rightarrow VV$ decays, the information on branching ratios and polarization fractions among various helicity amplitudes have been studied by many authors [1–4]. Through polarization studies, some underlying helicity structures of the decay mechanism are proclaimed. People find that the polarization fractions follow the naive counting rule, that is $f_L \sim 1 - O(m_V^2/m_B^2)$, $f_N \sim f_T \sim O(m_V^2/m_B^2)$, where $f_{L,N,T}$ denote the longitudinal, parallel, and perpendicular polarization fractions, respectively, and $m_B(m_V)$ is the $B(V)$ meson mass. But if the contributions from the factorizable emission amplitudes are suppressed for some decay modes, this counting rule might be modified to some extent even more dramatically by other contributions. For example, many anomalous longitudinal polarization fractions in the decays $B \rightarrow \rho K^*$, ϕK^* have been measured by experiments, which are about 50% [5], except that of the decay $B^- \rightarrow K^{*-}\rho^0$ with large value $(96_{-16}^{+6})\%$ [5] (the newer measurement is $(90 \pm 20)\%$ [6]). Whether a similar results also occurs in the decay modes $B \rightarrow a_1(1260)K^*$, $b_1(1235)K^*$ is worth researching. We know that $a_1(1260)$ has some similar behaviors as the vector meson, so one can expect that there should exist some similar characteristics in the branching ratios and the polarization fractions between the decays $B \rightarrow a_1(1260)K^*$ and $B \rightarrow \rho K^*$, where $a_1(1260)$ and ρ are scalar partners of each other, while this is not the case for $b_1(1235)$ because of its different characteristics in the decay constant and light-cone distribution amplitude (LCDA) compared with those of $a_1(1260)$. For example, the longitude decay constant is very small for the charged $b_1(1235)$ states and vanishes under the SU(3) limit. It is zero for the neutral $b_1^0(1235)$ state. While the transverse decay constant of $a_1(1260)$ vanishes under the SU(3) limit. In the isospin limit, the chiral-odd (-even) LCDAs of meson $b_1(1235)$ are symmetric (antisymmetric) under the exchange of quark and antiquark momentum fractions. It is just contrary to the symmetric behavior for $a_1(1260)$. In view of these differences, one can expect that there should exist very different results between $B \rightarrow a_1(1260)K^*$ and $B \rightarrow b_1(1235)K^*$. On the theoretical side, the decays $B \rightarrow a_1(1260)K^*$, $b_1(1235)K^*$ have been studied by Cheng and Yang in Ref. [7], where the branching ratios are very different with those calculated by the naive factorization approach [8]. To clarify such large differences is another motivation of this work. On the experimental side, only the upper limits for some of the considered decays can be available [9, 10].

In the following, $a_1(1260)$ and $b_1(1235)$ are denoted as a_1 and b_1 in some places for convenience. The layout of this paper is as follows. In Sec.II, we analyze these decay channels by using the PQCD approach. The numerical results and the discussions are

given in Sec.III. The conclusions are presented in the final part.

II. THE PERTURBATIVE QCD CALCULATION

The PQCD approach has been proved been an effective theory to handle hadronic B decays in many works [2, 3, 11, 12]. Because of taking into account the transverse momentum of the valence quarks in the hadrons, one will encounter double logarithm divergences when the soft and the collinear momenta overlap. Fortunately, these large double logarithm can be re-summed into the Sudakov factor [13]. There are also another type of double logarithms which arise from the loop corrections to the weak decay vertex. These double logarithms can also be re-summed and resulted in the threshold factor, which decreases faster than any other power of the momentum fraction in the threshold region, which removes the endpoint singularity. This factor is often parameterized into a simple form which is independent on channels, twists and flavors [14]. Certainly, when the higher order diagrams only suffer from soft or collinear infrared divergence, it is ease to cure by using the eikonal approximation [15]. Controlling these kinds of divergences reasonably makes the PQCD approach more self-consistent.

In the standard model, the related weak effective Hamiltonian H_{eff} mediating the $b \rightarrow s$ type transitions can be written as [16]

$$\mathcal{H}_{eff} = \frac{G_F}{\sqrt{2}} \left[\sum_{p=u,c} V_{pb} V_{ps}^* (C_1(\mu) O_1^p(\mu) + C_2(\mu) O_2^p(\mu)) - V_{tb} V_{ts}^* \sum_{i=3}^{10} C_i(\mu) O_i(\mu) \right]. \quad (1)$$

Here the function $Q_i(i = 1, \dots, 10)$ is the local four-quark operator and C_i is the corresponding Wilson coefficient. $V_{p(t)b}$, $V_{p(t)s}$ are the CKM matrix elements. The standard four-quark operators are defined as:

$$\begin{aligned} O_1^u &= \bar{s}_\alpha \gamma^\mu L u_\beta \cdot \bar{u}_\beta \gamma_\mu L b_\alpha, & O_2^u &= \bar{s}_\alpha \gamma^\mu L u_\alpha \cdot \bar{u}_\beta \gamma_\mu L b_\beta, \\ O_3 &= \bar{s}_\alpha \gamma^\mu L b_\alpha \cdot \sum_{q'} \bar{q}'_\beta \gamma_\mu L q'_\beta, & O_4 &= \bar{s}_\alpha \gamma^\mu L b_\beta \cdot \sum_{q'} \bar{q}'_\beta \gamma_\mu L q'_\alpha, \\ O_5 &= \bar{s}_\alpha \gamma^\mu L b_\alpha \cdot \sum_{q'} \bar{q}'_\beta \gamma_\mu R q'_\beta, & O_6 &= \bar{s}_\alpha \gamma^\mu L b_\beta \cdot \sum_{q'} \bar{q}'_\beta \gamma_\mu R q'_\alpha, \\ O_7 &= \frac{3}{2} \bar{s}_\alpha \gamma^\mu L b_\alpha \cdot \sum_{q'} e_{q'} \bar{q}'_\beta \gamma_\mu R q'_\beta, & O_8 &= \frac{3}{2} \bar{s}_\alpha \gamma^\mu L b_\beta \cdot \sum_{q'} e_{q'} \bar{q}'_\beta \gamma_\mu R q'_\alpha, \\ O_9 &= \frac{3}{2} \bar{s}_\alpha \gamma^\mu L b_\alpha \cdot \sum_{q'} e_{q'} \bar{q}'_\beta \gamma_\mu L q'_\beta, & O_{10} &= \frac{3}{2} \bar{s}_\alpha \gamma^\mu L b_\beta \cdot \sum_{q'} e_{q'} \bar{q}'_\beta \gamma_\mu L q'_\alpha, \end{aligned} \quad (2)$$

where α and β are the $SU(3)$ color indices; L and R are the left- and right-handed projection operators with $L = (1 - \gamma_5)$, $R = (1 + \gamma_5)$. The sum over q' runs over the quark fields that are active at the scale $\mu = O(m_b)$, i.e., ($q' \in \{u, d, s, c, b\}$). At leading order, there are eight types of single hard gluon exchange diagrams contributing to our considered decays, dividing into the emission type diagrams and the annihilation type diagrams, each type diagram including two factorizable ones and two nonfactorizable ones. Because of the limited space, we do not show these diagrams.

Combining the contributions from different diagrams, the total decay amplitudes for

these decays can be written as

$$\begin{aligned}
\sqrt{2}\mathcal{M}_j(\bar{K}^{*0}a_1^0) = & \xi_u(F_{eK^*}^{LL,j}a_2 + M_{eK^*}^{LL,j}C_2) - \xi_t \left[F_{eK^*}^{LL,j} \left(\frac{3C_7}{2} + \frac{C_8}{2} + \frac{3C_9}{2} + \frac{C_{10}}{2} \right) \right. \\
& - (F_{ea_1}^{LL,j} + F_{aa_1}^{LL,j}) \left(a_4 - \frac{a_{10}}{2} \right) + M_{eK^*}^{LL,j} \frac{3C_{10}}{2} + M_{eK^*}^{SP,j} \frac{3C_8}{2} \\
& - (M_{ea_1}^{LL,j} + M_{aa_1}^{LL,j}) \left(C_3 - \frac{1}{2}C_9 \right) - (M_{ea_1}^{LR,j} + M_{aa_1}^{LR,j}) \left(C_5 - \frac{1}{2}C_7 \right) \\
& \left. - (F_{ea_1}^{SP,j} + F_{aa_1}^{SP,j})(a_6 - \frac{1}{2}a_8) \right], \tag{3}
\end{aligned}$$

$$\begin{aligned}
\mathcal{M}_j(\bar{K}^{*0}a_1^-) = & \xi_u [M_{aa_1}^{LL,j}C_1 + F_{aa_1}^{LL,j}a_1] - \xi_t \left[F_{ea_1}^{LL,j} \left(a_4 - \frac{a_{10}}{2} \right) + F_{aa_1}^{LL,j} (a_4 + a_{10}) \right. \\
& + M_{ea_1}^{LL,j} \left(C_3 - \frac{1}{2}C_9 \right) + M_{aa_1}^{LL,j} (C_3 + C_9) + M_{ea_1}^{LR,j} \left(C_5 - \frac{1}{2}C_7 \right) \\
& \left. + M_{aa_1}^{LR,j} (C_5 + C_7) + F_{aa_1}^{SP,j}(a_6 + a_8) \right], \tag{4}
\end{aligned}$$

$$\begin{aligned}
\sqrt{2}\mathcal{M}_j(\bar{K}^{*-}a_1^0) = & \xi_u \left[F_{eK^*}^{LL,j}a_2 + M_{eK^*}^{LL,j}C_2 + M_{aa_1}^{LL,j}C_1 + F_{aa_1}^{LL,j}a_1 \right] - \xi_t \left[M_{eK^*}^{LL,j} \frac{3}{2}C_{10} \right. \\
& + M_{eK^*}^{SP,j} \frac{3}{2}C_8 + M_{aa_1}^{LL,j} (C_3 + C_9) + M_{aa_1}^{LR,j} (C_5 + C_7) \\
& \left. + F_{aa_1}^{LL,j} (a_4 + a_{10}) + F_{aa_1}^{SP,j}(a_6 + a_8) \right], \tag{5}
\end{aligned}$$

$$\begin{aligned}
\mathcal{M}_j(\bar{K}^{*-}a_1^+) = & \xi_u \left[F_{ea_1}^{LL,j}a_1 + M_{ea_1}^{LL,j}C_1 \right] - \xi_t \left[F_{ea_1}^{LL,j} (a_4 + a_{10}) + M_{ea_1}^{LL,j} (C_3 + C_9) \right. \\
& + M_{ea_1}^{LR,j} (C_5 + C_7) + M_{aa_1}^{LL,j} \left(C_3 - \frac{1}{2}C_9 \right) + M_{aa_1}^{LR,j} \left(C_5 - \frac{1}{2}C_7 \right) \\
& \left. + F_{aa_1}^{LL,j} \left(a_4 - \frac{1}{2}a_{10} \right) + F_{aa_1}^{SP,j} \left(a_6 - \frac{1}{2}a_8 \right) \right], \tag{6}
\end{aligned}$$

here $F_{ea_1}^{LL,j}$ denotes the amplitudes of the factorizable emission diagrams, where one can extract out the $B \rightarrow a_1$ transition form factor. If we replace the positions of a_1 and \bar{K}^* and will get the amplitudes $F_{eK^*}^{LL,j}$ and $F_{eK^*}^{SP,j}$. As for the amplitudes of non-factorizable emission diagrams, $M_{ea_1}^{LL,j}$ and $M_{ea_1}^{LR,j}$ are relevant to the considered decays. The amplitudes $M_{eK^*}^{LL,j}$ and $M_{eK^*}^{SP,j}$ are obtained by exchanging a_1 and \bar{K}^* in these non-factorizable emission diagrams. It is similar to the annihilation diagram amplitudes, where $F_{aa_1}^{LL,j}$ and $F_{aa_1}^{SP,j}$ are for the factorizable ones, $M_{aa_1}^{LL,j}$ and $M_{aa_1}^{LR,j}$ are for the non-factorizable ones. It is noticed that the upper labels LL , LR , and SP denote the $(V-A)(V-A)$, $(V-A)(V+A)$, and $(S-P)(S+P)$ currents, respectively, and j denotes three types of polarizations (one longitudinal and two transverses), and named as L, N, T . Limitations of space prevent us from giving the analytical expressions for these amplitudes. The combinations of the Wilson coefficients are defined as usual:

$$a_1(\mu) = C_2(\mu) + \frac{C_1(\mu)}{3}, a_2(\mu) = C_1(\mu) + \frac{C_2(\mu)}{3}, \tag{7}$$

$$a_i(\mu) = C_i(\mu) + \frac{C_{i+1}(\mu)}{3}, \quad i = 3, 5, 7, 9, \tag{8}$$

$$a_i(\mu) = C_i(\mu) + \frac{C_{i-1}(\mu)}{3}, \quad i = 4, 6, 8, 10. \tag{9}$$

The amplitudes for those decays involving the b_1 meson can be derived from the above expressions Eq.(4)-Eq.(6) by substituting the b_1 meson wave functions for a_1 ones.

III. NUMERICAL RESULTS AND DISCUSSIONS

For the wave function of the heavy B meson, we take [11]

$$\Phi_B(x, b) = \frac{1}{\sqrt{2N_c}} (\not{P}_B + m_B) \gamma_5 \phi_B(x, b). \quad (10)$$

Here only the contribution of Lorentz structure $\phi_B(x, b)$ is taken into account, since the contribution of the second Lorentz structure $\bar{\phi}_B$ is numerically small [17] and has been neglected. For the distribution amplitude $\phi_B(x, b)$ in Eq.(10), we adopt the following model:

$$\phi_B(x, b) = N_B x^2 (1-x)^2 \exp\left[-\frac{M_B^2 x^2}{2\omega_b^2} - \frac{1}{2}(\omega_b b)^2\right], \quad (11)$$

where ω_b is a free parameter, and taken as $\omega_b = 0.4 \pm 0.04$ GeV in numerical calculations, and $N_B = 91.745$ is the normalization factor for $\omega_b = 0.4$. This is the same wave functions as in Ref.[11], which is a best fit for most of the measured hadronic B decays.

In these decays, both the longitudinal and the transverse polarizations are involved for the vector meson K^* . Its distribution amplitudes are defined as

$$\begin{aligned} \langle K^*(P, \epsilon_L^*) | \bar{q}_{2\beta}(z) q_{1\alpha}(0) | 0 \rangle &= \frac{1}{\sqrt{2N_c}} \int_0^1 dx e^{ixp \cdot z} [m_{K^*} \not{\epsilon}_L^* \phi_{K^*}^t(x) + \not{\epsilon}_L^* \not{P} \phi_{K^*}^t(x) \\ &\quad + m_{K^*} \phi_{K^*}^s(x)]_{\alpha\beta}, \end{aligned} \quad (12)$$

$$\begin{aligned} \langle K^*(P, \epsilon_T^*) | \bar{q}_{2\beta}(z) q_{1\alpha}(0) | 0 \rangle &= \frac{1}{\sqrt{2N_c}} \int_0^1 dx e^{ixp \cdot z} [m_{K^*} \not{\epsilon}_T^* \phi_{K^*}^v(x) + \not{\epsilon}_T^* \not{P} \phi_{K^*}^T(x) \\ &\quad + m_{K^*} i \epsilon_{\mu\nu\rho\sigma} \gamma_5 \gamma^\mu \epsilon_T^{*v} n^\rho v^\sigma \phi_{K^*}^a(x)]_{\alpha\beta}, \end{aligned} \quad (13)$$

where $n(v)$ is the unit vector having the same (opposite) direction with the moving of the vector meson and x is the momentum fraction of q_2 quark. The upper (sub)leading twist wave functions can be parameterized as

$$\phi_{K^*}(x) = \frac{f_{K^*}}{2\sqrt{2N_c}} \phi_{\parallel}(x), \quad \phi_{K^*}^T(x) = \frac{f_{K^*}^T}{2\sqrt{2N_c}} \phi_{\perp}(x), \quad (14)$$

$$\phi_{K^*}^t(x) = \frac{f_{K^*}^T}{2\sqrt{2N_c}} h_{\parallel}^{(t)}(x), \quad \phi_{K^*}^s(x) = \frac{f_{K^*}^T}{2\sqrt{4N_c}} \frac{d}{dx} h_{\parallel}^{(s)}(x), \quad (15)$$

$$\phi_{K^*}^v(x) = \frac{f_{K^*}}{2\sqrt{2N_c}} g_{\perp}^{(v)}(x), \quad \phi_{K^*}^a(x) = \frac{f_{K^*}}{8\sqrt{2N_c}} \frac{d}{dx} g_{\perp}^{(a)}(x), \quad (16)$$

where

$$\phi_{\parallel, \perp} = 6x(1-x) \left[1 + 3a_{1K^*}^{\parallel, \perp} t + 3/2 a_{2K^*}^{\parallel, \perp} (5t^2 - 1) \right], \quad (17)$$

$$h_{\parallel}^{(t)}(x) = 3t^2, \quad h_{\parallel}^{(s)}(x) = 6x(1-x), \quad (18)$$

$$g_{\perp}^{(a)}(x) = 6x(1-x), \quad g_{\perp}^{(v)}(x) = 3/4(1+t^2). \quad (19)$$

TABLE I: Decay constants and Gegenbauer moments for K^* , a_1 and b_1 (in MeV). The values are taken at $\mu = 1$ GeV.

f_{K^*} 209 ± 2	$f_{K^*}^T$ 165 ± 9	f_{a_1} 238 ± 10	$f_{b_1}^T$ -180 ± 8
$a_1^\parallel(K^*)$ 0.03 ± 0.02	$a_1^\perp(K^*)$ 0.04 ± 0.03	$a_2^\parallel(K^*)$ 0.11 ± 0.09	$a_2^\perp(K^*)$ 0.10 ± 0.08
$a_2^\parallel(a_1(1260))$ -0.02 ± 0.02	$a_1^\perp(a_1(1260))$ -1.04 ± 0.34	$a_1^\parallel(b_1(1235))$ -1.95 ± 0.35	$a_2^\perp(b_1(1235))$ 0.03 ± 0.19

For the distribution amplitudes of the axial-vectors $a_1(b_1)$, they have the same format as those of K^* meson except the factor $i\gamma_5$ from the left hand:

$$\begin{aligned}
\langle A(P, \epsilon_L^*) | \bar{q}_{2\beta}(z) q_{1\alpha}(0) | 0 \rangle &= \frac{i\gamma_5}{\sqrt{2N_c}} \int_0^1 dx e^{ixp \cdot z} [m_A \not{\epsilon}_L^* \phi_A(x) + \not{\epsilon}_L^* \not{P} \phi_A^t(x) + m_A \phi_A^s(x)]_{\alpha\beta}, \\
\langle A(P, \epsilon_T^*) | \bar{q}_{2\beta}(z) q_{1\alpha}(0) | 0 \rangle &= \frac{i\gamma_5}{\sqrt{2N_c}} \int_0^1 dx e^{ixp \cdot z} [m_A \not{\epsilon}_T^* \phi_A^v(x) + \not{\epsilon}_T^* \not{P} \phi_A^T(x) \\
&\quad + m_A i \epsilon_{\mu\nu\rho\sigma} \gamma_5 \gamma^\mu \epsilon_T^{*v} n^\rho v^\sigma \phi_A^a(x)]_{\alpha\beta},
\end{aligned} \tag{20}$$

where A represents a_1 and b_1 . Their (sub)leading twist wave functions have also the same parameter formats with those of K^* , which can be gotten by replacing K^* with A in Eq.(14~ 16). The corresponding functions $\phi(x)$, $h(x)$, $g(x)$ for axial-vector are written as

$$\phi_{\parallel, \perp} = 6x(1-x) \left[a_0^{\parallel, \perp} + 3a_1^{\parallel, \perp} t + \frac{3a_2^{\parallel, \perp}}{2} (5t^2 - 1) \right], \tag{21}$$

$$h_\parallel^{(t)}(x) = 3a_0^\perp t^2 + \frac{3}{2} a_1^\perp t (3t^2 - 1), h_\parallel^{(s)}(x) = 6x(1-x)(a_0^\perp + a_1^\perp t), \tag{22}$$

$$g_\perp^{(a)}(x) = 6x(1-x)(a_0^\parallel + a_1^\parallel t), g_\perp^{(v)}(x) = \frac{3}{4} a_0^\parallel (1 + t^2) + \frac{3}{2} a_1^\parallel t^3, \tag{23}$$

where the zeroth Gegenbauer moments $a_0^\perp(a_1) = a_0^\parallel(b_1) = 0$ and $a_0^\parallel(a_1) = a_0^\perp(b_1) = 1$. Here $t = 2x - 1$, and other decay constants and Gegenbauer moments are listed in Table I.

The following input parameters are also used in our numerical calculations [19, 20]:

$$f_B = 190 \text{ MeV}, M_B = 5.28 \text{ GeV}, M_W = 80.41 \text{ GeV}, \tag{24}$$

$$\tau_{B^\pm} = 1.638 \times 10^{-12} \text{ s}, \tau_{B^0} = 1.525 \times 10^{-12} \text{ s}, \tag{25}$$

$$|V_{ub}| = 3.89 \times 10^{-3}, |V_{tb}| = 1.0, \gamma = (67.2 \pm 3.9)^\circ \tag{26}$$

$$|V_{us}| = 0.2252, |V_{ts}| = 38.7 \times 10^{-3}. \tag{27}$$

The matrix element \mathcal{M}_j of the operators in the weak Hamiltonian have been given in previous section, which are rewritten as

$$M_j = V_{ub} V_{us}^* T_j - V_{tb} V_{ts}^* P_j = V_{ub} V_{us}^* T_j (1 + z_j e^{i(\gamma + \delta_j)}), \tag{28}$$

TABLE II: Branching ratios (in units of 10^{-6}) for the decays $B \rightarrow a_1(1260)K^*$ and $B \rightarrow b_1(1235)K^*$. In our results, the errors for these entries correspond to the uncertainties from ω_B , the QCD scale $\Lambda_{QCD}^{(4)}$ and the threshold resummation parameter c , respectively. For comparison, we also listed the results predicted by QCDF approach [7] and the naive factorization approach [8].

	This work	[7]	[8]
$\bar{B}^0 \rightarrow a_1^+ K^{*-}$	$9.9^{+1.6+0.4+3.7}_{-1.1-0.6-3.7}$	$10.6^{+5.7+31.7}_{-4.0-8.1}$	0.92
$\bar{B}^0 \rightarrow a_1^0 \bar{K}^{*0}$	$7.1^{+1.5+0.4+3.1}_{-0.9-0.6-3.1}$	$4.2^{+2.8+15.5}_{-1.9-4.2}$	0.64
$B^- \rightarrow a_1^- \bar{K}^{*0}$	$10.8^{+2.0+0.7+4.6}_{-1.4-0.8-4.6}$	$11.2^{+6.1+31.9}_{-4.4-9.0}$	0.51
$B^- \rightarrow a_1^0 K^{*-}$	$4.8^{+0.6+0.2+1.6}_{-0.5-0.3-1.6}$	$7.8^{+3.2+16.3}_{-2.5-4.3}$	0.86
$\bar{B}^0 \rightarrow b_1^+ K^{*-}$	$18.0^{+3.3+1.3+6.3}_{-2.6-2.3-6.3}$	$12.5^{+4.7+20.1}_{-3.7-9.0}$	0.32
$\bar{B}^0 \rightarrow b_1^0 \bar{K}^{*0}$	$9.6^{+2.1+1.0+3.8}_{-1.5-1.1-3.8}$	$6.4^{+2.4+8.8}_{-1.7-4.8}$	0.15
$B^- \rightarrow b_1^- \bar{K}^{*0}$	$23.0^{+4.5+2.3+8.4}_{-3.5-2.9-8.4}$	$12.8^{+5.0+20.1}_{-3.8-9.6}$	0.18
$B^- \rightarrow b_1^0 K^{*-}$	$10.6^{+1.9+0.7+3.4}_{-1.5-1.4-3.4}$	$7.0^{+2.6+12.0}_{-2.0-4.8}$	0.12

where γ is the Cabibbo-Kobayashi-Maskawa weak phase angle, defined via $\gamma = \arg[-\frac{V_{tb}V_{ts}^*}{V_{ub}V_{us}^*}]$. δ_j is the relative strong phase between the tree and the penguin amplitudes, which are denoted as " T_j " and " P_j ", respectively. The term z_j describes the ratio of penguin to tree contributions and is defined as

$$z_j = \left| \frac{V_{tb}V_{ts}^*}{V_{ub}V_{us}^*} \right| \left| \frac{P_j}{T_j} \right|. \quad (29)$$

In the same way, it is easy to write decay amplitude $\overline{\mathcal{M}}_j$ for the corresponding conjugated decay mode:

$$\overline{\mathcal{M}}_j = V_{ub}^* V_{us} T_j - V_{tb}^* V_{ts} P_j = V_{ub}^* V_{us} T_j (1 + z_j e^{i(-\gamma+\delta_j)}). \quad (30)$$

So the CP-averaged branching ratio for each considered decay is defined as

$$\begin{aligned} \mathcal{B} &= \frac{G_F^2 \tau_B}{32 \hbar \pi m_B} (|\mathcal{M}_j|^2 + |\overline{\mathcal{M}}_j|^2) / 2 \\ &= \frac{G_F^2 \tau_B}{32 \hbar \pi m_B} |V_{ub} V_{us}^*|^2 \left[T_L^2 (1 + 2z_L \cos \gamma \cos \delta_L + z_L^2) \right. \\ &\quad \left. + 2 \sum_{i=N,T} T_i^2 (1 + 2z_i \cos \gamma \cos \delta_i + z_i^2) \right]. \end{aligned} \quad (31)$$

Like the decays of B to two vector mesons, there are also 3 types of helicity amplitudes, so corresponding to 3 types of z_j and δ_j , respectively. It is easy to see that the dependence of decay width on δ and γ is more complicated compared with that for the decays of B to two pseudoscalar mesons.

Using the input parameters as specified in this section, it is easy to get the branching ratios for the considered decays, which are listed in Table II, where the first error comes

from the uncertainty in the B meson shape parameter $\omega_b = 0.40 \pm 0.04$ GeV, the second error is induced by the hard scale-dependent varying from $\Lambda_{QCD}^{(4)} = 0.25 \pm 0.05$, and the last one is from the threshold resummation parameter c varying from 0.3 to 0.4.

In our predictions, the branching ratio of the decay $\bar{B}^0 \rightarrow a_1^0 \bar{K}^{*0}$ is larger than that of the decay $B^- \rightarrow a_1^0 K^{*-}$, it is mainly induced by the amplitudes of the factorizable emission diagrams, F_{ea_1} and F_{eK^*} , have contrary interference effects between these two decays : constructive for the decay $a_1^0 \bar{K}^{*0}$, destructive for the decay $a_1^0 K^{*-}$. So the decay $\bar{B}^0 \rightarrow a_1^0 \bar{K}^{*0}$ receives a larger real part for the penguin amplitudes. Though the decay $B^- \rightarrow a_1^0 K^{*-}$ has much larger contributions from tree amplitudes, which are CKM suppressed and can not change the branching ratio too much. In order to characterize the contribution from tree operators and the symmetry breaking effects between B^- and \bar{B}^0 mesons, it is useful to define the two ratios:

$$R_1 = \frac{\mathcal{B}(B^- \rightarrow a_1^- \bar{K}^{*0})}{\mathcal{B}(\bar{B}^0 \rightarrow a_1^+ K^{*-})} \times \frac{\tau_{\bar{B}^0}}{\tau_{B^-}}, \quad R_2 = \frac{\mathcal{B}(B^- \rightarrow b_1^0 K^{*-})}{\mathcal{B}(\bar{B}^0 \rightarrow b_1^+ K^{*-})} \times \frac{\tau_{\bar{B}^0}}{\tau_{B^-}}. \quad (32)$$

If one neglects the tree operators and the electro-weak penguins, the ratios obey the following limits

$$R_1 = 1, R_2 = 0.5. \quad (33)$$

Here our predictions of these two ratios are 1.02 and 0.55, respectively. The results predicted by QCDF approach are 0.98 and 0.52, respectively. If the future data for R_1 have large deviation from our value, the contributions from electro-weak penguin operators might give an important affect, for the contribution from tree operators can not change the branching ratio of $\bar{B}^0 \rightarrow a_1^+ K^{*-}$ too much. If the future data for R_2 have large deviation from our value, some mechanism beyond factorization even from new physics might give an important affect, because the factorization formulae between $\bar{B}^0 \rightarrow b_1^+ K^{*-}$ and $B^- \rightarrow b_1^0 K^{*-}$ are exactly the same by considering the neutral b_1^0 meson decay constant vanishing.

Compared with other results: From Table II, One can find that our predictions are consistent well with the QCDF results within (large) theoretical errors, while in stark disagreement with the naive factorization approach, where the nonfactorizable effects are described by the effective number of colors N_c^{eff} . For some decays, where the contributions from the emission diagrams are dominated or the branching ratios have a strong dependence on the correlative form factors, the naive factorization approach can give a reasonable prediction, while for the decays, where the annihilation diagrams play an important role, this approach would expose some disadvantages. On the experimental side, BarBar has been searched the decays $B \rightarrow a_1^- \bar{K}^{*0}, b_1 K^*$ and set the upper limits on their branching ratios ranging from 3.3 to 8.0×10^{-6} at the 90% confidence level [9, 10]. Certainly, these upper limits are obtained by assuming that $\mathcal{B}(a_1^\pm \rightarrow \pi^+ \pi^- \pi^\pm) = \mathcal{B}(a_1^\pm \rightarrow \pi^0 \pi^0 \pi^\pm)$ and $\mathcal{B}(a_1^\pm(b_1^\pm) \rightarrow \rho^0(\omega) \pi^\pm) = 1$. Furthermore, the background signals may give an important effort on these upper limits, such as the background decay channel $B \rightarrow a_2 \bar{K}^{*0}$ in studying of the decay $B \rightarrow a_1 \bar{K}^{*0}$. In view of these disagreements, we strongly suggest that the LHCb and the forthcoming Super-B experiments to accurately measure these decays modes.

From Table III, we find that the polarization characters for the decays $B \rightarrow a_1 K^*$ and $B \rightarrow b_1 K^*$ are very different: the transverse polarization amplitudes have almost equal

TABLE III: Longitudinal polarization fraction (f_L) and two transverse polarization fractions (f_{\parallel} , f_{\perp}) for decays $B \rightarrow a_1(1260)K^*$ and $B \rightarrow b_1(1235)K^*$. In our results, the uncertainties come from ω_B , the QCD scale $\Lambda_{QCD}^{(4)}$ and the threshold resummation parameter c . The results of f_L predicted by the QCDF approach are also displayed in parentheses for comparison.

	$f_L(\%)$	$f_{\parallel}(\%)$	$f_{\perp}(\%)$
$\bar{B}^0 \rightarrow a_1^+ K^{*-}$	$48.9^{+5.1+7.4+4.9}_{-4.7-8.0-4.9} (37^{+39}_{-29})$	$26.1^{+2.5+3.8+2.6}_{-2.8-4.1-2.6}$	$25.0^{+2.2+3.8+2.3}_{-2.3-3.5-2.3}$
$\bar{B}^0 \rightarrow a_1^0 \bar{K}^{*0}$	$59.6^{+4.7+7.7+4.3}_{-4.9-7.8-4.3} (23^{+45}_{-19})$	$20.2^{+2.6+3.8+2.2}_{-2.5-3.8-2.2}$	$20.2^{+2.3+4.0+2.1}_{-2.2-3.5-2.1}$
$B^- \rightarrow a_1^- \bar{K}^{*0}$	$50.3^{+5.1+8.6+5.0}_{-4.9-9.9-5.0} (37^{+48}_{-37})$	$24.1^{+2.6+5.0+2.5}_{-2.7-3.7-2.5}$	$25.6^{+2.3+5.0+2.5}_{-2.4-4.9-2.5}$
$B^- \rightarrow a_1^0 K^{*-}$	$49.0^{+3.3+6.2+4.7}_{-4.3-6.2-4.7} (52^{+41}_{-42})$	$25.5^{+2.3+0.0+2.4}_{-2.5-2.5-2.4}$	$25.5^{+2.0+3.2+2.2}_{-2.2-3.7-2.2}$
$\bar{B}^0 \rightarrow b_1^+ K^{*-}$	$95.9^{+0.1+1.1+0.0}_{-0.1-1.3-0.0} (82^{+18}_{-41})$	$1.1^{+0.2+0.4+0.2}_{-0.0-0.2-0.2}$	$3.0^{+0.0+0.9+0.2}_{-0.1-0.7-0.2}$
$\bar{B}^0 \rightarrow b_1^0 \bar{K}^{*0}$	$95.4^{+0.1+1.0+0.1}_{-0.1-1.4-0.1} (79^{+21}_{-74})$	$0.9^{+0.0+0.2+0.4}_{-0.0-0.2-0.4}$	$3.7^{+0.1+1.2+0.3}_{-0.1-0.8-0.3}$
$B^- \rightarrow b_1^- \bar{K}^{*0}$	$96.2^{+0.0+0.9+0.1}_{-0.0-1.7-0.1} (79^{+21}_{-74})$	$1.0^{+0.0+0.3+0.3}_{-0.0-0.3-0.3}$	$2.8^{+0.0+0.9+0.2}_{-0.0-0.6-0.2}$
$B^- \rightarrow b_1^0 K^{*-}$	$96.5^{+0.0+0.8+0.1}_{-0.1-1.3-0.1} (82^{+16}_{-26})$	$0.7^{+0.1+0.2+0.2}_{-0.0-0.1-0.2}$	$2.8^{+0.0+0.9+0.3}_{-0.0-0.6-0.3}$

values with (even a little stronger than) the longitudinal polarization ones for the former, while the longitudinal polarization states are dominated for the latter. It seems that the anomalous polarizations occurring in decays $B \rightarrow \phi K^*, \rho K^*$ also happen in $B \rightarrow a_1 K^*$ decays, while do not happen in $B \rightarrow b_1 K^*$ decays. Here we also find that the contributions from the annihilation diagrams are very important to the final polarization fractions for $B \rightarrow a_1 K^*$ decays: If these contributions are neglected, the longitudinal polarization fraction of the decay $B^- \rightarrow a_1^0 K^{*-}$ becomes 98.8%, those of $\bar{B}^0 \rightarrow a_1^+ K^{*-}, a_1^0 \bar{K}^{*0}$ increase to about 90%, that of the decay $B^- \rightarrow a_1^- \bar{K}^{*0}$ changes from 50.3% to 70.0%. While the longitudinal polarizations of decays $B \rightarrow b_1 K^*$ only have a very small decrease by neglecting the annihilation type contributions except that of the decay $B^- \rightarrow b_1^- \bar{K}^{*0}$, which has a little large reduction, changing from 96.2% to 86%. In a word, the longitudinal polarizations of decays $B \rightarrow b_1 K^*$ are not very sensitive to the annihilation type contributions compared with those of $B \rightarrow a_1 K^*$ decays.

Now we turn to the evaluations of the CP-violating asymmetries in PQCD approach. Here we only research the decays $B \rightarrow b_1 K^*$, where the transverse polarization fractions are very small and range from 3.8 to 5.2%. It is easy to see that for these $b_1 K^*$ decay modes, the contributions from the transverse polarizations are very small, so we neglected them in our calculations. Using Eq.(28) and Eq.(30), one can get the expression for the direct CP-violating asymmetry:

$$\mathcal{A}_{CP}^{dir} = \frac{|\overline{\mathcal{M}}|^2 - |\mathcal{M}|^2}{|\mathcal{M}|^2 + |\overline{\mathcal{M}}|^2} = \frac{2z_L \sin \alpha \sin \delta_L}{(1 + 2z_L \cos \alpha \cos \delta_L + z_L^2)}.$$

Using the input parameters and the wave functions as specified in this section, one can find the PQCD predictions (in units of 10^{-2}) for the direct CP-violating asymmetries of

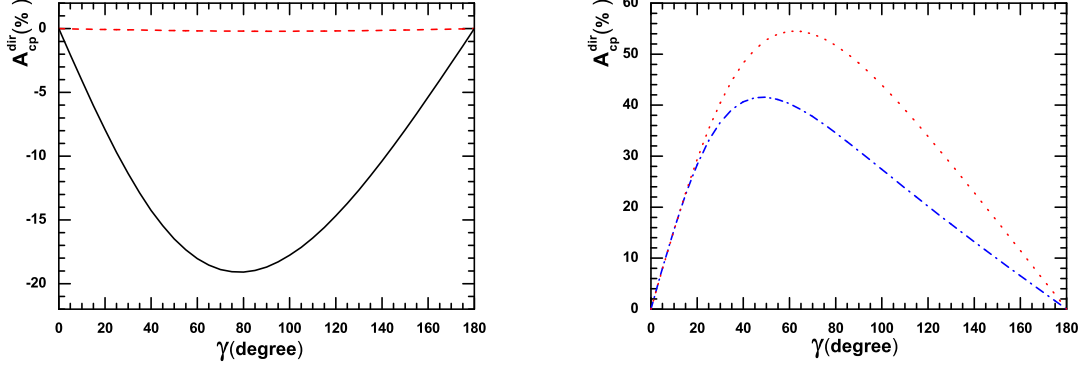


FIG. 1: The dependence of the branching ratios on the Cabibbo-Kobayashi-Maskawa angle γ . The left (right) panel is for the decays $B \rightarrow a_1(b_1)K^*$. The dotted line represents the decays $B^- \rightarrow a_1^0(b_1^0)K^{*-}$, the solid line represents the decays $\bar{B}^0 \rightarrow a_1^0(b_1^0)\bar{K}^{*0}$, the dashed line is for the decays $B^- \rightarrow a_1^-(b_1^-)\bar{K}^{*0}$, the dot-dashed line is for the decays $\bar{B}^0 \rightarrow a_1^+(b_1^+)K^{*-}$.

the considered decays:

$$\mathcal{A}_{CP}^{dir}(\bar{B}^0 \rightarrow b_1^+ K^{*-}) = 38.5_{-1.7-7.4-4.5}^{+1.2+8.8+4.5}, \quad (34)$$

$$\mathcal{A}_{CP}^{dir}(B^- \rightarrow b_1^0 K^{*-}) = 54.3_{-1.7-6.7-4.4}^{+0.9+7.8+4.4}, \quad (35)$$

$$\mathcal{A}_{CP}^{dir}(\bar{B}^0 \rightarrow b_1^0 \bar{K}^{*0}) = -18.7_{-1.3-0.3-1.8}^{+2.0+0.7+1.8}, \quad (36)$$

$$\mathcal{A}_{CP}^{dir}(B^- \rightarrow b_1^- \bar{K}^{*0}) = -0.18_{-0.28-0.00-0.33}^{+0.23+0.47+0.33}, \quad (37)$$

where the errors are induced by the uncertainties of B meson shape parameter $\omega_b = 0.4 \pm 0.04$, the hard scale-dependent varying from $\Lambda_{QCD}^{(4)} = 0.25 \pm 0.05$, and the threshold resummation parameter c varying from 0.3 to 0.4. In Fig.1, we show the Cabibbo-Kobayashi-Maskawa angle γ dependence of the direct CP-violating asymmetries of upper four decays. It is particularly noteworthy that our predictions about the direct CP asymmetries of these decays are consistent well with the QCDF results [21] :

$$\mathcal{A}_{CP}^{dir}(\bar{B}^0 \rightarrow b_1^+ K^{*-}) = (44_{-58}^{+3})\%, \quad (38)$$

$$\mathcal{A}_{CP}^{dir}(B^- \rightarrow b_1^0 K^{*-}) = (60_{-73}^{+6})\%, \quad (39)$$

$$\mathcal{A}_{CP}^{dir}(\bar{B}^0 \rightarrow b_1^0 \bar{K}^{*0}) = (-17_{-10}^{+21})\%, \quad (40)$$

$$\mathcal{A}_{CP}^{dir}(B^- \rightarrow b_1^- \bar{K}^{*0}) = (2_{-2}^{+0})\%, \quad (41)$$

where the error comes from the parameters $\rho_{A,H}$ and arbitrary phases $\phi_{A,H}$. These are phenomenological parameters to cure the endpoint divergences in the amplitudes for the annihilation and hard spectator scattering diagrams.

IV. CONCLUSION

In this paper, by using the decay constants and the light-cone distribution amplitudes derived from QCD sum-rule method, we research $B \rightarrow a_1 K^*, b_1 K^*$ decays in PQCD factorization approach and find that

- Our predictions for the branching ratios are consistent well with the QCDF results within errors, but larger than the naive factorization approach calculation values. On the experimental side, some primary upper limit values are inexplicable. In view of these disagreements, we strongly suggest that the LHCb and the forthcoming Super-B experiments can further accurately measure these decays modes.
- The anomalous polarizations occurring in decays $B \rightarrow \phi K^*, \rho K^*$ also happen in decays $B \rightarrow a_1 K^*$, while do not happen in decays $B \rightarrow b_1 K^*$. Here the contributions from the annihilation diagrams play an important role to explain the larger transverse polarizations in decays $B \rightarrow a_1 K^*$, while are not sensitive to the polarizations in decays $B \rightarrow b_1 K^*$.
- Our predictions for the direct CP-asymmetries agree well with the QCDF results within errors. The decays $\bar{B}^0 \rightarrow b_1^+ K^{*-}, B^- \rightarrow b_1^0 K^{*-}$ have larger direct CP-asymmetries, which could be measured by the present LHCb and the forthcoming Super-B experiments.

Acknowledgment

This work is partly supported by the National Natural Science Foundation of China under Grant No. 11147004, 11347030, by the Program of the Youthful Key Teachers in University of Henan Province under Grant No. 001166, and by Foundation of Henan University of Technology under Grant No. 2009BS038.

-
- [1] Y. Li, C. D. Lu, Phys. Rev. D **73**, 014024 (2006).
 - [2] H. W. Huang, *et al.*, Phys. Rev. D **73**, 014011 (2006).
 - [3] A. Ali, *et al.*, Phys. Rev. D **76**, 074018 (2007).
 - [4] M. Beneke, J. Rohrer, D.S. Yang, Phys. Lett. B **768**, 51 (2007).
 - [5] E. Barberio, *et al.*, [Heavy Flavor Averaging Group], arXiv:0808.1297 [hep-ex] (2008) and online update <http://www.slac.stanford.edu/xorg/hfag>.
 - [6] B. Aubert, *et al.*, [BABAR Collaboration], Phys. Rev. Lett. **97**, 201801 (2006).
 - [7] H. Y. Cheng, K. C. Yang, Phys. Rev. D **78**, 094001 (2008).
 - [8] G. Calderon, J.H. Munoz and C.E. Vera, Phys. Rev. D **76**, 094019 (2007), arXiv:hep-ph/0705.1181.
 - [9] B. Aubert, *et al.*, [BABAR Collaboration], Phys. Rev. D **82**, 091101 (2010), arXiv:hep-ex/0808.0579v1.
 - [10] B. Aubert, *et al.*, [BABAR Collaboration], Phys. Rev. D **80**, 051101 (2009), arXiv:hep-ex/0907.3485v1.

- [11] Y. Y. Keum, H. N. Li, A. I. Sanda, Phys. Lett. B **504**, 6 (2001); Phys. Rev. D **63**, 054008 (2001); C. D. Lü, K. Ukai, M. Z. Yang, Phys. Rev. D **63**, 074009 (2001); Y. Y. Keum, H. N. Li, Phys. Rev. D **63**, 074006 (2001); C. D. Lü, M. Z. Yang, Eur. Phys. J. C **23**, 275 (2002).
- [12] H. n. Li, S. Mishima, A. I. Sanda, Phys. Rev. D **72**, 114005 (2005).
- [13] H. n. Li and B. Tseng, Phys. Rev. D **57**, 443 (1998).
- [14] H. n. Li and K. Ukai, Phys. Lett. B **555**, 197 (2003).
- [15] H. n. Li and H. L. Yu, Phys. Rev. D **53**, 2480 (1996).
- [16] G. Buchalla, A. J. Buras, M. E. Lautenbacher, Rev. Mod. Phys., 1996, **68**: 1125.
- [17] C.D. Lu and M.Z. Yang, Eur. Phys. J. C **28**, 515 (2003).
- [18] Z.Q. Zhang, Phys. Rev. D **85**, 114005 (2012).
- [19] K. Nakamura, *et al.*, [Particle Data Group], J. Phys. G**37**, 481 (2010).
- [20] CKMfitter Group, <http://ckmfitter.in2p3.fr>.
- [21] K. C. Yang, arXiv:hep-ph/0810.1782.